A&A 500, L29–L32 (2009)
DOI: 10.1051/0004-6361/200912296

Astronomy & Astrophysics

Letter to the Editor

Intermittency of interstellar turbulence: parsec-scale coherent structure of intense, velocity shear⋆

P. Hily-Blant[1] and E. Falgarone[2]

[1] LAOG, CNRS & Université Joseph Fourier, UMR 5571, 414 rue de la Piscine, BP 53, 38041 Grenoble Cedex 09, France
e-mail: pierre.hilyblant@obs.ujf-grenoble.fr
[2] LRA/LERMA, CNRS & École normale supérieure & Observatoire de Paris, UMR 8112, 24 rue Lhomond, 75231 Paris Cedex 05, France

Received 7 April 2009 / Accepted 12 May 2009

ABSTRACT

Aims. Benefitting from the duality of turbulence (random versus coherent motions), we search for coherent structures in the turbulent velocity field of molecular clouds, anticipating their importance in cloud evolution.
Methods. We analyse a large map (40′ by 20′) obtained with the HERA multibeam receiver (IRAM-30 m telescope) in a high latitude cloud of the Polaris Flare at unprecedented spatial (11″) and spectral (0.05 km s^{-1}) resolution for the ^{12}CO(2−1) line.
Results. We find that two parsec-scale components of velocities differing by ∼2 km s^{-1}, share a narrow interface (<0.15 pc) that appears to be an elongated structure of intense velocity-shear, ∼15 to 30 km s^{-1} pc^{-1}. The locus of the extrema of line–centroid-velocity increments (E-CVI) in that field follows this intense-shear structure as well as that of the ^{12}CO(2−1) high-velocity line wings. The tiny spatial overlap in projection of the two parsec-scale components implies that they are sheets of CO emission and that discontinuities in the gas properties (CO enrichment and/or increase in gas density) occur at the position of the intense velocity shear.
Conclusions. These results identify spatial and kinematic coherence on scales of between 0.03 pc and 1 pc. They confirm that the departure from Gaussianity of the probability density functions of E-CVIs is a powerful statistical tracer of the intermittency of turbulence. They provide support for a link between large-scale turbulence, its intermittent dissipation rate and low-mass dense core formation.

Key words. ISM: clouds – ISM: magnetic fields – ISM: kinematics and dynamics – ISM: molecules – turbulence

1. Introduction

Because it is supersonic, magnetized, and develops in a multi-phase medium, interstellar turbulence is expected to differ from turbulence in laboratory flow experiments or in state-of-the-art numerical simulations, e.g., Chanal et al. (2000) for experiments in gaseous helium and Mininni et al. (2006a) or Alexakis et al. (2007) for MHD simulations. Nonetheless, it may carry some universal properties of turbulence, such as space-time intermittency (for a review see Anselmet et al. 2001). The behaviour of turbulence dissipation is of particular interest to star formation. In a series of papers (Hily-Blant & Falgarone 2007; Hily-Blant et al. 2008, hereafter Paper I and Paper II), we have shown that the ^{12}CO(1−0) line–centroid-velocity increments (CVI) in translucent molecular gas have non-Gaussian statistics that are more pronounced on small scales. The extreme CVI (E-CVI) responsible for the non-Gaussian tails of their probability density functions (*pdf*) form elongated coherent structures over 0.8 pc. These structures have been tentatively identified with regions of intense velocity-shear[1] and enhanced local dissipation rate, based on their thermal, dynamical, and chemical properties. These pure velocity-structures do not follow those of dense gas: they tend to be parallel to the magnetic field orientation, they are associated with gas warmer ($T_{\rm kin}$ > 25 K) than the bulk of the gas, and they bear chemical signatures of a warm chemistry that is not driven by UV photons (Falgarone et al. 2006; Godard et al. 2009). In one of these E-CVI structures, Plateau de Bure Interferometre (PdBI) observations disclose several substructures of intense velocity-shear at scales as small as 6 milliparsec (mpc) (Falgarone et al. 2009, hereafter FPH09). This suggests that turbulent molecular clouds harbour coherent velocity-shear structures on scales of between 6 mpc to 800 mpc.

We increase our dynamic range by a factor of 8 compared with Paper II, by mapping a four times larger area in the Polaris Flare with twice the spatial resolution. We aimed to further explore the range of scales over which the spatial coherence of these intense-shear structures is found. These are the first large-scale observations performed at high-angular resolution and high spectral resolution in translucent gas. The observations and the results are described in Sects. 2 and 3. We briefly discuss the possible interpretation and nature of these structures by comparison with numerical simulations (Sect. 4).

2. Observations

Observations of the ^{12}CO(2−1) line were carried out at the IRAM-30m telescope with the 1.3 mm multibeam heterodyne receiver HERA (Schuster et al. 2004) during August 2007 and

⋆ Based on observations carried out with the IRAM-30 m telescope. IRAM is supported by INSU-CNRS/MPG/IGN.

[1] In the following, "shear" is used instead of gradient to emphasize that the observations provide cross-derivatives of the line–centroid-velocities (CV) (i.e., the displacement, in the plane-of-the-sky (POS), is perpendicular to the projection axis of the velocities).

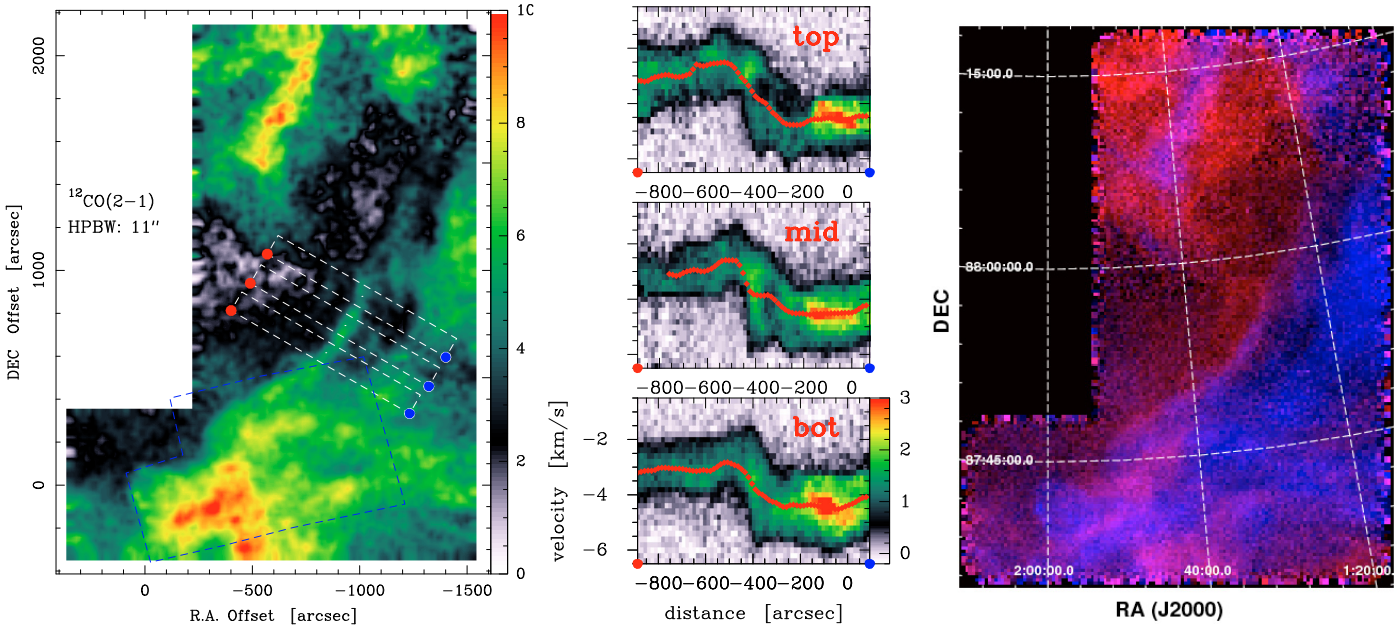

Fig. 1. *Left*: integrated intensity map (K km s^{-1}, T_A^*scale) smoothed to 15″. The white dashed boxes show the areas used to build the average $p-v$ cuts (*right panels*). The blue rectangle (dashed line) delineates the previous field of Paper I. *Middle*: $p-v$ cuts in the 3 boxes shown in *left panel*, centered at offsets (–841″, 615″), (–933″, 744″) and (–1012″, 881″) (T_A^* scale, distance measured in ″ with arbitrary origin). The line CV are shown in red. *Right*: ^{12}CO(2−1) integrated intensity in two adjacent velocity ranges: [−6.5: − 3.5] km s^{-1} in blue and [−3.5: − 0.5] km s^{-1} in red. At a distance of 150 pc, 20′ corresponds to 0.9 pc.

January 2008, in good weather conditions. The map covers 0.3 deg^2 and consists of 9 submaps of 10′ × 10′, each of which was observed in two orthogonal scanning directions to minimize striping due to gain or atmosphere variations. The final map encompasses the field observed by Falgarone et al. (1998) and in Paper I (indicated as a dashed box in Fig. 1) and is of area ∼2 × 1 pc at the adopted distance of the source (150 pc). Data were acquired in the powerful on-the-fly (OTF) frequency-switched mode (4″ s^{-1} scanning velocity, 1 s time sampling, 4″ spatial sampling in both directions, 13.8 MHz frequency throw), using the VESPA autocorrelator facility as backends. A total of 1.5×10^6 raw spectra was recorded in 80 h of telescope time with a spectral resolution of 0.05 km s^{-1}. Data were reduced with the new `CLASS90` software optimized for OTF (Hily-Blant et al. 2005). Each spectrum was corrected for the instrumental response by subtracting a linear baseline, then convolved by a Gaussian kernel (1/3 *HPBW*), and gridded onto a regular grid with 0.5*HPBW* sampling. The final data cube was then smoothed to spatial and velocity resolutions of 15″ and 0.1 km s^{-1}, respectively, to improve the signal-to-noise ratio. The typical rms in each final pixel was 1σ = 0.5 K in 0.1 km s^{-1} channels.

3. Results

3.1. Space and velocity maps

The ^{12}CO(2−1) integrated emission is displayed in Fig. 1 (left panel) with three position-velocity ($p-v$) diagrams (middle panels) compiled along the NE-SW boxes shown. A sharp variation in velocity, from ∼−3 km s^{-1} to ∼−5 km s^{-1} (from NE to SW) occurs over a layer thinner than a few 100″ in projection. The right panel of Fig. 1 displays the integrated emission in two adjacent velocity intervals, at high (HV) [–3.5, –0.5] km s^{-1} and low velocity (LV) [–6.5, –3.5] km s^{-1}, and highlights the remarkable characteristic of that field: the edges of the LV and HV components follow each other closely in projection over more than ∼1 pc. It is then unlikely that these components are unrelated pieces of gas along the line of sight: they must be in contact.

The second remarkable characteristic of that field is the following: while the emission in both the LV and HV components is extended, their spatial overlap (the pink areas in the right panel of Fig. 1, also evident in the $p-v$ diagrams) is limited to narrow filamentary regions in projection. It is visible mostly between δ = 87°45′ and 88° (thus over ∼1 pc), where it does not split into several substructures. If the LV and HV components were parsec-scale volumes, their interface would appear thin over ∼1 pc only if viewed edge-on (within ±5° for a projected size less than one tenth of its real size), a possibility that we exclude on statistical grounds. We therefore infer that the ^{12}CO(2−1) HV and LV components are *layers* rather than *volumes* and that their interface is 1-dimensional rather than 2-dimensional. This ensures that along any viewing angle the two extended velocity components are visible as a narrow interface.

The slope of the variations in the line CV drawn on the $p-v$ diagrams provides a measurement of the velocity shear between the two components. On each cut shown, there is an average shear of ≈13 km s^{-1} pc^{-1} (a velocity variation of 2 km s^{-1} over ≈0.15 pc). Steeper slopes are also visible and provide locally higher shears up to 30 km s^{-1} pc^{-1} (1 km s^{-1} over 0.03 pc) in the middle cut. These values are more than one order of magnitude higher (within the uncertainties due to projections) than the average value of 1 km s^{-1} pc^{-1} estimated on the parsec scale in molecular clouds (Goldsmith & Arquilla 1985). The velocity field therefore significantly deviates, on small scales, from predictions based on the generally adopted scaling laws in molecular clouds. If velocity fluctuations on a scale l increase in amplitude as $\delta v_l \propto l^{1/2}$, velocity shears should increase by no more than $33^{1/2} \approx 5.7$ between 1 pc and 0.03 pc.

A closer inspection of the $p-v$ diagrams shows that (i) the sharpest variations in the line CV occur between two line

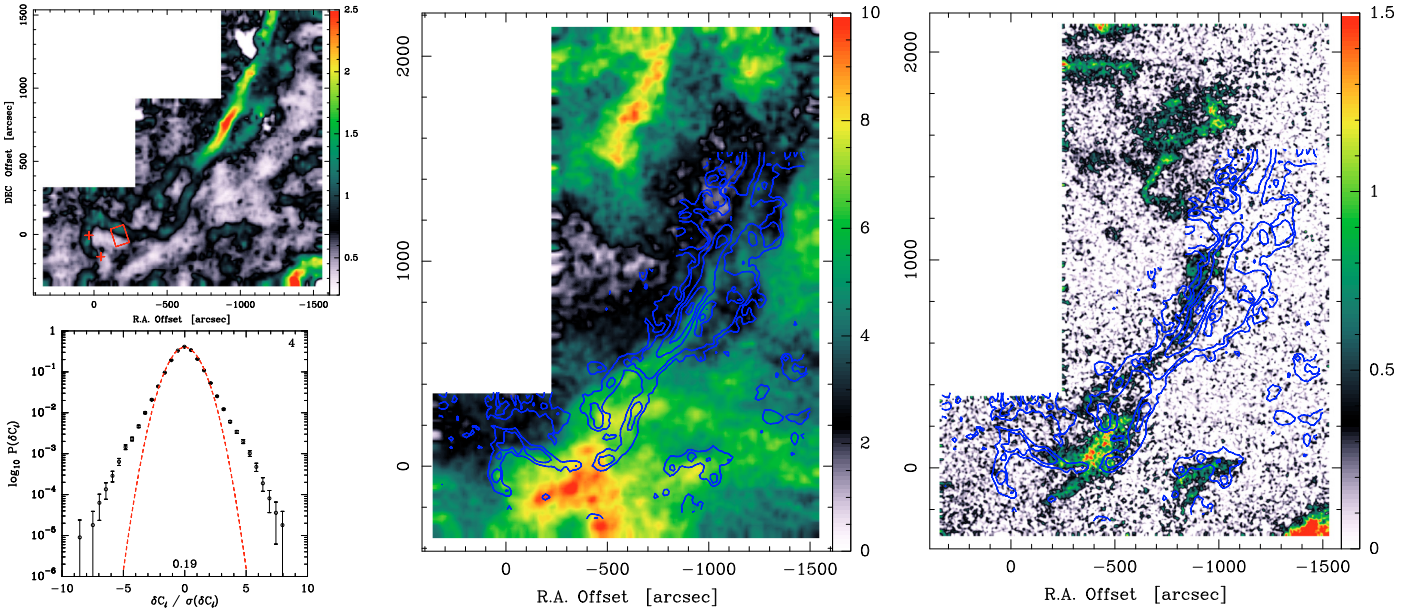

Fig. 2. *Left*: map of the CVI (top panel, colour scale in km s^{-1}) computed for a lag of 4 pixels or 60″, and normalized *pdf* (circles, *bottom left panel*) compared with a Gaussian distribution (σ = 0.19 km s^{-1}, red). The red crosses (*top panel*) indicate the position of the dense cores from Heithausen (2002). The rectangle delineates the PdBI field of Falgarone et al. (2009). *Middle*: E-CVI (blue contours) overplotted on the integrated intensity of Fig. 1. *Right*: E-CVI (blue contours) overplotted on the intensity integrated in the red wing interval [–2: –0.5] km s^{-1} (Hily-Blant & Falgarone 2007).

wings appearance (above −2.0 km s^{-1} for the HV wing and below −5.5 km s^{-1} for the LV wing); (ii) the separation between the LV and HV wings steepens from top (0.1 pc) to bottom (0.03 pc); and (iii) the layer of largest velocity shear coincides with the lane of enhanced ^{12}CO(2−1) emission visible in Fig. 1 at the centre of each cut.

3.2. Distribution of E-CVI

Following Lis et al. (1996), Pety & Falgarone (2003) and Paper II, we have compiled the *pdf* (see Fig. 2) of ^{12}CO(2−1) CVI over the entire field. The statistics of our data analysis is significantly higher than previous work. The probability density in the most extreme bins reaches 10^{-5}. Figure 2 displays the locus of the E-CVI. It is remarkable that the thin structure delineated by the ^{12}CO(2−1) E-CVI in the SE area (blue box of Fig. 1) is so similar to that obtained with the same method applied to a much smaller sample observed in a different transition, ^{12}CO(1−0) (Paper II). The E-CVI structure is the high-angular resolution view of the structure obtained with the same statistical analysis performed on KOSMA maps of the field (*HPBW* = 120″) and shown in Fig. 12 of Paper II.

The E-CVI structure does not follow the peaks of the ^{12}CO(2−1) line integrated emission. Instead, it coincides, over the ∼1 pc region discussed in Sect. 3.1, with the narrow interface of the HV and LV components i.e., the intense velocity shear (Fig. 2, centre), and follows in detail the thin elongated structure in the extreme velocity range [−2.0, −0.5] km s^{-1}, which is that of the red line wings (Fig. 2, right). This association between CO linewings and intense velocity shears extends the findings of Paper II to higher resolution and over a wider scale.

These properties of the locus of E-CVI support unambiguously, for the first time, the proposition of Paper II that the E-CVI trace intense, velocity shears in turbulent gas and that the extreme variations in the line CV are driven by the appearance/disappearance of line wings on small scales. It is also the first observational proof of the early conjecture of Falgarone & Phillips (1990) that the broad CO line wings trace the intermittency of turbulence in molecular clouds. These results clarify, at least in the case of translucent clouds, the controversy about the origin of small-scale CV variations expected to be caused primarily by density fluctuations, line-of-sight projections, and radiative transfer (Esquivel et al. 2007; Miville-Deschênes et al. 2003; Levrier 2004).

Finally, this E-CVI structure is coherent over ∼2 pc, while its thickness is as small as 0.03−0.15 pc. Its aspect ratio is therefore ∼70−15, and its length seems to be limited by the size of the map (see the longer structure computed from the KOSMA data in Paper II). We also note that the E-CVI structure separates into multiple branches in several areas, in particular around the offsets (−1000″, 800″) and (−700″, 500″).

4. Discussion

In the following, we propose a chemical and dynamical scenario that can account for the observational results.

4.1. What is the nature of the interface?

The interface is primarily an intense velocity-shear. The $p-v$ diagrams show that this velocity shear corresponds to a discontinuity in the CO flow: the HV (LV) component is not detected above ∼0.5 K in the SW (NE) of the shear. The flows undetected in the ^{12}CO(2−1) line are either CO-poor and/or too dilute to excite the transition. In this framework, we observe the yield of a strain developing in a gas undetected in the ^{12}CO(2−1) line: the gas that we detect (denser and/or richer in CO) is generated in the 1-dimensional intense-shear interface and spread in the POS by motions whose velocity cannot be measured. This scenario naturally produces the two components of the large velocity-shear, with sharp edges closely following each other over ∼1 pc and little overlap in projection *for any viewing angle*.

The intense-shear structure may however belong to a shock of unknown velocity in the POS. We have searched for SiO(2−1) line emission as a chemical shock signature within this structure and found no emission above a significant low threshold $3\sigma = 5$ mK corresponding, in the optically thin case, to a tiny SiO column density of about 10^{10} cm^{-2}. Hence, there is no chemical signature of C-shocks faster than 20 km s^{-1} detected on the scale of 0.03 pc (Gusdorf et al. 2008). However, we cannot exclude a weak C-shock component ($v_S \leq 2$ km s^{-1}) in the POS that would produce the density enhancement and/or the CO enrichment in the gas required to explain the non-detection in the ^{12}CO(2−1) line of the gas before it enters the shear layer. This would be consistent with the sub- to trans-Alfvénic nature of the turbulent motions in that field (see Paper II). The solenoidal contribution to the interface (2 km s^{-1}) would exceed the possible compressive one (≤2 km s^{-1}), in agreement with Federrath et al. (2009), who found that our observed statistical properties of turbulence in the Polaris Flare are in good agreement with solenoidal forcing on large scales. This result is similar to the findings of Mininni et al. (2006a) that the stronger the shear on large scales, the more intense the intermittency of velocity increments on small scales.

4.2. A plausible link with the dense cores

The above findings are similar to those inferred from PdBI observations (FPH09) of the small (1′ by 2′) field shown in Fig. 2 (left). Velocity shears as intense as 500 km s^{-1} pc^{-1} are detected over distances of 6 mpc, at the edge of CO structures of velocities differing by several km s^{-1}. The PdBI field is close to two low-mass dense cores (Heithausen 2002), interestingly located at the tip of the E-CVI structure (Fig. 2, left).

Since the viscous dissipation rate of turbulence is proportional to the square of the rate-of-strain (Landau & Lifschitz 1987), it is tempting to interpret the large increase in the velocity-shear, from 30 km s^{-1} pc^{-1} (Fig. 1) to 500 km s^{-1} pc^{-1} in the PdBI field, as being caused by the development of an instability in the large-scale shear. The growth of the instability divides the shear into small-scale and more intense shears, thus increasing the local dissipation rate of turbulence by two-orders of magnitude. Clustering of small-scale structures of high strain-rate magnitude (and therefore large dissipation) into structures of inertial extension have been found in numerical simulations of incompressible HD (Moisy & Jiménez 2004) and MHD turbulence (Mininni et al. 2006b). One may then speculate that these bursts of dissipation eventually lead to the formation of low-mass dense cores largely devoid of turbulent energy, after evolution of the gas that remains to be understood.

5. Conclusions

We have detected a 1-dimensional structure of intense velocity shear (∼15 to 30 km s^{-1} pc^{-1}), coherent over ∼1 pc of thickness between only 0.03 and 0.15 pc. This remarkable structure follows the distribution of extreme ^{12}CO(2−1) line-wings and coincides partly with the locus of E-CVIs in the field. These findings support our previous claim that, in translucent molecular clouds, E-CVIs are tracers of extreme velocity shears in interstellar turbulence, as are the broad CO line wings.

This shear structure is proposed to be the source of *layers* of CO-rich dense gas in a CO-poor (and/or dilute) gas component experiencing the strain and not seen in ^{12}CO(2−1). The shear is likely to be the site of enhanced turbulent dissipation. We cannot exclude an undetected shock component in the POS.

In conjunction with the PdBI results of FPH09, these results highlight the coupling between small and large scales in interstellar turbulence, over a dynamic range never before reached, i.e., from 6 mpc to more than 1 pc. They support a framework in which trans-Alfvénic (but supersonic) turbulence dissipates primarily in intense shear layers connecting the large-scales to mpc scales (or below).

We speculate that turbulence dissipation has been proceeding for a longer time at the southern tip of the E-CVI structure than in the northern part, leading to the formation of the two dense cores.

Acknowledgements. The authors thank M. Heyer for his clarifying and perceptive report on the original version of this Letter. We are grateful to C. Thum and H. Wiesemeyer from IRAM for their unfailing support to the HERA facility. The authors acknowledge the hospitality of the Kavli Institute for Theoretical Physics (Grant No. PHY05-51164).

References

Alexakis, A., Mininni, P. D., & Pouquet, A. 2007, New J. Phys., 9, 298
Anselmet, F., Antonia, R. A., & Danaila, L. 2001, Planet. Space Sci., 49, 1177
Chanal, O., Chabaud, B., Castaing, B., & Hébral, B. 2000, Eur. Phys. J. B, 17, 309
Esquivel, A., Lazarian, A., Horibe, S., et al. 2007, MNRAS, 381, 1733
Falgarone, E., & Phillips, T. G. 1990, ApJ, 359, 344
Falgarone, E., Panis, J.-F., Heithausen, A., et al. 1998, A&A, 331, 669
Falgarone, E., Pineau Des Forêts, G., Hily-Blant, P., & Schilke, P. 2006, A&A, 452, 511
Falgarone, E., Pety, J., & Hily–Blant, P. 2009, A&A, accepted
Federrath, C., Duval, J., Klessen, R. S., Schmidt, W., & Mac Low, M. M. 2009, A&A, submitted, [arXiv:0905.1060]
Godard, B., Falgarone, E., & Pineau des Forêts, G. 2009, A&A, 495, 847
Goldsmith, P. F., & Arquilla, R. 1985, in Protostars and Planets II, ed. D. C. Black, & M. S. Matthews, 137
Gusdorf, A., Pineau Des Forêts, G., Cabrit, S., & Flower, D. R. 2008, A&A, 490, 695
Heithausen, A. 2002, A&A, 393, L41
Hily-Blant, P., & Falgarone, E. 2007, A&A, 469, 173
Hily-Blant, P., Pety, J., & Guilloteau, S. 2005, CLASS evolution: I. Improved OTF support, Tech. rep., IRAM
Hily-Blant, P., Falgarone, E., & Pety, J. 2008, A&A, 481, 367
Landau, L. D., & Lifschitz, E. M. 1987, Fluid Mechanics (Pergamon Press)
Levrier, F. 2004, A&A, 421, 387
Lis, D. C., Pety, J., Phillips, T. G., & Falgarone, E. 1996, ApJ, 463, 623
Miville-Deschênes, M.-A., Levrier, F., & Falgarone, E. 2003, ApJ, 593, 831
Mininni, P. D., Alexakis, A., & Pouquet, A. 2006a, Phys. Rev. D, 74, 016303
Mininni, P. D., Pouquet, A. G., & Montgomery, D. C. 2006b, Phys. Rev. L., 97, 244503
Moisy, F., & Jiménez, J. 2004, J. Fluid Mech., 513, 111
Pety, J., & Falgarone, E. 2003, A&A, 412, 417
Schuster, K.-F., Boucher, C., Brunswig, W., et al. 2004, A&A, 423, 1171